

Fleming, J.W., Reed, M.D., Zegers, E.J.P., Williams, B.A., and Sheinson, R.S., "Extinction Studies of Propane/Air Counterflow Diffusion Flames: The Effectiveness of Aerosols," *Proceedings of the 1998 Halon Options Technical Working Conference*, Albuquerque, pp. 403-414 1998.

Extinction Studies of Propane/Air Counterflow Diffusion Flames: The Effectiveness of Aerosols

James W. Fleming, Mark D. Reed^a, Eric J.P. Zegers^b, Bradley A. Williams, and Ronald S. Sheinson

NAVAL RESEARCH LABORATORY

Navy Technology Center for Safety and Survivability

Combustion Dynamics Section, Code 6185, Washington, DC 20375-5342 USA

(202) 767-2065 Fax (202) 767-1716 E-mail: fleming@code6185.nrl.navy.mil

ABSTRACT

We have examined the fire suppression effectiveness of solid aerosols as suitable halon replacements. Experiments were performed in a counterflow diffusion burner, consisting of two 1 cm i.d. tubes separated by 1 cm. Aerosols were delivered to propane/air flames in the air flow. Both sodium bicarbonate (NaHCO_3) and potassium bicarbonate (KHCO_3) powders were examined. The NaHCO_3 and KHCO_3 powders were separated into various size groupings ($< 38 \mu\text{m}$, $38\text{--}45 \mu\text{m}$, $45\text{--}53 \mu\text{m}$, $53\text{--}63 \mu\text{m}$, and $63\text{--}75 \mu\text{m}$) using a commercial sieving system. The agent delivery system incorporated a variable orifice for gross adjustment of the delivery rate, and a variable frequency vibration unit for fine adjustments and to maintain powder flow. Light scattering using a modulated HeNe laser beam and a lock-in amplifier was used to monitor the amount of powder exiting the air tube and entering the flame. Extinction concentrations were determined for each agent sample as a function of the strain rate of the uninhibited flame. In general, suppression effectiveness increased with decreasing particle size or increasing strain rate for the size range studied. Potassium powders were ~ 2.5 times by weight more effective than sodium powders. The suppression effectiveness of these powders as a function of particle size can be interpreted using a simplified model of the behavior of particles in counterflowing streams.

BACKGROUND

The list of suitable halon alternatives for fire suppression includes aerosols. Both liquid droplets and solid particles have shown promise as potential replacements. Small particles of alkali metal salts have been observed to be more effective on a mass basis than Halon 1301 [1,2]. The most common alkali metal salt agents in use are sodium bicarbonate (NaHCO_3) and potassium bicarbonate

This research is sponsored primarily as part of the Department of Defense's Next-Generation Fire Suppression Technology Program, co-funded by the DoD Strategic Environmental Research and Development Program. We acknowledge the U. S. Naval Sea Systems Command 03R16 for partial financial support and Adam Chattaway of Kidde International for furnishing the sieved powder samples.

^a Center for Firesafety Studies, WPI; WPI/NRL Intern 1996-1997.

Current address: Rolf Jensen and Associates, Inc., Walnut Creek, CA 94598

^b NRL/NRC Postdoctoral Research Fellow October 1997 - present.

(KHCO_3). NaHCO_3 is widely used in fire extinguishers because of its low cost. Both agents also have markets in explosion protection, and in such applications as paint spray booths, fuel filling stations and restaurant cooking areas. In addition to high efficiency, the powders have many other advantages, including low toxicity and corrosivity. They also have minimal impact on the environment as they have zero ozone depletion or global warming potential.

However, the powder left by the dry chemicals following suppression remains a drawback, limiting their application to areas that can tolerate the residue. Decreased visibility during application is also a concern. Furthermore, in many applications, the particles must remain suspended in the fire threat area sufficiently long to eliminate the chances of reignition. The agent must also flow around objects to extinguish obstructed fires in a similar manner to gaseous agents. For conventional sized extinguishing powders (i.e. 20-100 μm), the majority of the particles are too massive and not capable of suspension for extended periods of time. Therefore, short particle suspension times are another limitation of current bicarbonate agents, especially for applications requiring a total flooding agent.

The questions of flow and suspension are currently being addressed by searching for ways to generate smaller fire-fighting particulates. Micron size particles of potassium bicarbonate powder have been developed [3] and are being tested in Europe for use in scenario specific applications [4]. Pyrotechnic particle generation methods can also yield micron sized aerosols and are being evaluated for use in fire suppression applications [1].

In addition to improved flow and suspension characteristics, smaller particles have also been associated with increased fire suppression effectiveness of powders on a mass basis. Effectiveness has been found to increase with decreasing particle size [5-9], leading many researchers to suggest that this is due to the ability of smaller particles to decompose and vaporize more readily.

In the 1980's, Ewing, Hughes, and Carhart [10] began looking at the flame extinguishing properties of dry chemicals and developed an empirical relationship to predict the flame suppression effectiveness of liquid, gaseous, and solid agents. They showed that suppression of a methane fire was achieved predominantly by heat extraction from the flame by means of heat capacity sinks and endothermic reaction sinks, such as vaporization, dissociation, and decomposition. They concluded that the extinguishing potential of an agent could be predicted from its thermodynamic properties. In later tests, Ewing et al. [11] extinguished heptane pan fires in a 420 liter test chamber. Both NaHCO_3 and KHCO_3 powders, formed of particles ranging in size from below 10 μm to 110 μm , were applied to the fires via a pressurized discharge nozzle. For each powder, a critical size was observed at which a near discontinuous change in effectiveness occurred. Above or below this critical value, effectiveness was found to increase only slightly with decreasing particle size. In a companion effort, Fischer and Leonard [8] performed extinction studies on 21 agents in a premixed flame. They also observed a distinct transition region separating effective and ineffective particle sizes. Similar experiments were performed by Chattaway et al. [3] in evaluating the efficiency of aerosol particulates.

Several opposed flow flame inhibition studies have also been conducted with powders. Hamins et al. [2] used a counterflow burner to study extinction of heptane and JP-8 flames by 13 gaseous agents and sodium bicarbonate powders. These powders were separated in three nominal size ranges: 0-10 μm , 10-20 μm , and 20-30 μm . Results were not reported for powders above 30 μm . They concluded that the 0-10 μm size range was the most effective, followed by the 20-30 μm and then the 10-20 μm range. No explanation for the non-monotonic behavior of effectiveness with size was proposed. Knuth, Ni, and Seeger [12] studied the flame inhibition effectiveness of several

dry chemicals, including KHCO_3 and NaHCO_3 , solely in the $38\mu\text{m}$ to $43\mu\text{m}$ size range, by adding powders to a counterflow diffusion flame and observing their impact on species and temperature profiles. The powders were then ranked in order of reaction-inhibition effectiveness. KCl was found to be the most effective inhibitor, followed by $\text{NH}_4\text{H}_2\text{PO}_4$, KHCO_3 , NaHCO_3 , and finally Al_2O_3 .

The experiments described in the current study were also performed in a counterflow diffusion flame configuration. This experimental configuration was chosen because the flames produced in a counterflow burner are near one-dimensional, and as such are more easily characterized and modeled. The present study addresses the particle size issue over a larger range of diameters than that previously investigated in counterflow flames. Flame extinction is also studied at various flame strain rates in order to investigate the effects of strain rate on suppression effectiveness.

EXPERIMENTAL

The counterflow flame configuration used to conduct the powder extinction experiments is illustrated in Figure 1. A flame can be established in the region between the two tubes where the opposed fuel and oxidizer flows meet and diffuse. Counterflow flames can be characterized in terms of a strain rate, the maximum velocity gradient on the oxidizer side of the flame. Extinction is achieved when the air and fuel flow rates are such that the velocity gradient exceeds a critical value referred to as the *extinction strain rate*. Suppression agents act to lower this critical value.

The particular counterflow diffusion burner [13] employed in the powder experiments consisted of two axisymmetric 1 cm i.d. burner tubes separated by 1 cm. Air was supplied through the top tube and propane through the bottom tube. Prior to any testing, the burner chamber and tubes were cleaned to remove any excess powder. The flame was lit and the flows adjusted to produce a predetermined strain rate. Powder suppression effectiveness was then determined by ramping up the powder loading until the flame extinguished.

Uninhibited propane/air flames were found to possess an extinction strain rate of 560 s^{-1} . Powder suppression effectiveness was therefore evaluated in flames whose uninhibited strain rates were below this limit. Flames with one of three initial strain rates were used: 180, 305, and 475 s^{-1} , referred to as low, medium, and high. The flow rates corresponding to these conditions are provided in Table 1. The experimental strain rates for the uninhibited flames were evaluated using Laser-Doppler velocimetry (LDV) following the procedure outlined by Fisher, Williams, and Fleming [14].

Unlike previously studied methane/air flames, the propane/air flames were bowl-shaped, with a flat horizontal burning region centered along the burner axis. The position of this flat region was approximately midway between the two tubes, as determined by the momenta of the flows. Upon extinction, the flat horizontal region of the flame disappeared, but the upper curved region remained stabilized to the upper burner tube. The flame continued to burn in the annular configuration even after the flow of powder was stopped, as the flame had attached and stabilized itself on the upper tube. The air and fuel flow rates were then decreased to destabilize the annular flame and recover the original flame structure. This process was repeated for a given powder and given flow conditions until 8 to 10 extinction points had been collected. The procedure was then repeated for the same powder at the remaining two strain rates. Duplicate testing occurred for all of the samples. Extinction strain rates determined with the centerline extinction criterion have been shown to be valid and are consistent with other studies [14]. Total extinguishment of the propane/air flames was only achieved when these flames were sufficiently shocked by dumping excessive amounts of powder on them.

For all of the powder suppression runs conducted, the powder was injected and mixed into the air stream from above the flame to simulate total flooding applications. The powder delivery system provided a steady flow of agent with controlled variability from 10 to 300 mg/min. This airtight system incorporated a glass metering valve with an adjustable orifice, formed of a brass rod inserted into a matching tapered glass tube. By changing the size of the orifice, coarse adjustment of the powder loading could be achieved. A tee above the orifice was used to introduce the powder. To maintain powder flow, the metering system had to be vibrated. The vibration mechanism consisted of a piece of teflon which made contact with a rotating wheel of variable frequency. The teflon was fastened to the glass tube near the orifice, using a hose clamp through which vibrations were communicated to the metering valve. Fine adjustment of the powder delivery rate were obtained by varying the rotation frequency of the wheel.

To collect accurate extinction loading measurements, powder flow rates had to be monitored. Monitoring involved positioning a modulated helium-neon laser beam perpendicular to the flow of powder just below the top tube exit; and evaluating the light scattered at 90° by the powder using a collection lens, a photomultiplier tube and a lock-in amplifier. The relationship between scattered light intensity and powder flow rate was determined by collecting and weighing powder in the absence of a flame. Because particle scattering intensity depended on air velocity and size distribution of the particles forming the powder, a calibration had to be obtained for each powder size, at each flow rate tested.

During an extinction run, the scattered light intensity was continuously recorded as powder loading was increased. The extinction loading could then be determined by probing the intensity trace at the exact time of flame extinction. To determine this time, a portion of the flame image appearing on the video screen used to follow the experiment was monitored by a fiber optic. Extinction of the flame was evidenced by a dramatic change in light intensity from the video signal. The addition of powder to the flame dramatically increased the excited C_2 emission from the flame. Therefore, a suitable optical filter was used to block this overwhelming emission from the video monitor.

Extinction experiments were conducted with sodium bicarbonate ($NaHCO_3$) and potassium bicarbonate ($KHCO_3$). Silica (2% by mass) was added to the powder samples as a drying additive. Both powders seemed to flow very freely with almost no agglomeration noticed. The powders were mechanically sieved into size ranges of $<38 \mu m$, 38-45 μm , 45-53 μm , 53-63 μm , and 63-75 μm . Nevertheless, in the case of $KHCO_3$, representative photomicrographs of the various fractions produced revealed a large percentage of very small particles in all of them.

RESULTS AND DISCUSSION

Extinction mass concentration measurements are provided in Table 2. These extinction loadings are plotted in Figure 2 as a function of measured uninhibited flame strain rate, holding bin size constant. They are replotted in Figure 3 as a function of average particle size, holding strain rate constant. The average particle size is taken as the arithmetic mean of the bin size limits. Figures 2a and 3a are for $NaHCO_3$. Figures 2b and 3b are for $KHCO_3$. In general, the extinction mass concentration varies inversely with the strain rate of the flame, and directly with the particle size of the powder.

For all three strain rates, the evolution of effectiveness with particle size in the size range studied is continuous, as opposed to exhibiting the jumps in effectiveness and plateauing behavior observed in the pan fire tests of Ewing et al. [7]. In those tests, agent effectiveness was found to

increase gradually as particle diameter decreased until a critical diameter was reached. At this diameter, a dramatic increase in the flame suppression efficiency occurred, with the effectiveness remaining constant with particle size below the limit. The limit sizes reported for NaHCO_3 and KHCO_3 are $16\ \mu\text{m}$ and $22\ \mu\text{m}$, respectively. In the present study, the most dramatic increase in performance with decreasing size was observed in the low strain rate flame. For both NaHCO_3 and KHCO_3 , as shown in Figures 3a and 3b, little gain in effectiveness is achieved by decreasing particle size below $40\ \mu\text{m}$.

Insight into the dependence of suppression effectiveness on strain rate and size can be gained by looking at how these parameters determine where given particles decompose in a particular flame. As the particles exit the top tube of the burner, they tend to position themselves at different locations in the counterflowing field, based on their size and mass, and the magnitude of the velocity field. Li, Libby, and Williams [15] mathematically examined the behavior of droplets in an opposed flow field. Large droplets fall through the stagnation plane and escape the flow field, as long as the drag forces which are attained are not sufficient to match the effects of gravity. Small droplets follow the gas velocity streamlines. Slightly larger droplets penetrate the stagnation plane, are “pushed back” by the opposing flow, and exhibit a decaying oscillatory behavior near the stagnation plane. The amplitude for this oscillation is a function of particle size. Lentati and Chelliah [16] calculated different trajectories for water droplets as a function of size in a counterflow burner. These calculations are only valid for the particular conditions (e.g. strain rate, spherical droplets) modeled, but non-spherical particles will behave in a qualitatively similar manner. The calculations indicate that the amplitude of the oscillations is essentially zero for a $30\ \mu\text{m}$ droplet. Thus, for smaller droplets, the resulting oscillatory trajectories are essentially confined to a plane.

The proximity of the oscillatory “plane” to the stagnation plane depends on particle size and strain rate, but not on the original direction of the particle trajectory. Figure 4 shows the axial positions of the oscillatory planes relevant to bicarbonate spheres, 10 to $70\ \mu\text{m}$ in diameter, in a potential non-reacting counterflow field model of the experimental medium strain rate flame studied. The drag forces on the particles are assumed to obey Stokes law. The 0 and $1\ \text{cm}$ positions correspond to the propane and air tube exits, respectively. Fully developed pipe flow centerline velocities, calculated from experimental flow rates and tube cross-sections, were used as model exit velocities, yielding a stagnation plane at $0.39\ \text{cm}$. Also shown in the figure are calculated axial temperature and O, H, and OH radical profiles for the propane/air flame at the medium strain rate. Whether the powder is introduced in the upper or lower flow, gravity dictates that the particles will asymptotically oscillate in planes below the stagnation plane. Smaller particles will lie closer to this plane.

The location of the oscillatory plane becomes significant if the opposing flows support a flame. Stoichiometry dictates that the propane/air diffusion flame will be located on the air side, as shown in Figure 4. With air and agent supplied from the top, and propane from the bottom, the flame will always lie above the stagnation plane. All particles will pass through the flame and those particles within a certain range of diameters (~ 20 to $60\ \mu\text{m}$ for the low strain rate flows) will oscillate below the stagnation plane, and hence below the flame. As the particles decompose, they get smaller such that they will migrate closer to the stagnation plane, never reaching the flame center.

With propane supplied from the top, and air and agent from the bottom, the flame will lie below the stagnation plane on the air side. In this configuration, some of the particles will be able to position themselves where flame temperature is at a maximum. Due to the higher temperature,

greater decomposition of the powder should occur at this location, leading to higher alkali metal atom concentrations closer to the maxima of key flame radicals. Significant interaction of the powders with the flame is therefore expected when trajectories are such that particle residence times near the maximum temperature region are large. Following this analysis, an optimum initial particle size for suppression in this flame configuration could exist. Since the distance of the flame center to the stagnation plane is a function of strain rate, the optimum particle size would also be expected to vary with strain rate. Experiments will be conducted to verify these hypotheses when the problem of supplying powders from the bottom tube is resolved. With top delivery, particles are essentially dropped; particles of any size can be delivered to the flame. However, with bottom delivery, particles can not be conveniently supplied at a fixed low air flow rate, since large particles require larger entrainment flow velocities than smaller ones.

The exact mode in which alkali metal bicarbonates act to inhibit flames is still not completely understood. Powders add a great deal of heat capacity to the flame. Solid particles are often effective infrared radiators as well, leading to cooling of the flame zone through radiation. Free radical scavenging processes involving either the solid surface of the particles (heterogeneous reactions) or gaseous by-products of agent decomposition (homogeneous reactions) have also been postulated to inhibit the combustion process [8-10]. Catalytic reactions would involve the metal atom (e.g. Na, K), and would proceed as $A + R + M \rightarrow AR + M$ followed by $AR + R' \rightarrow A + RR'$ where A is the metal atom, R and R' are H, O, or OH, and M is a third body. These reactions are exothermic and add heat to the flame. However, under conditions of favorable thermochemistry, radical scavenging inhibits the flame more than the additional heat promotes it. The possibility of catalytic recombination on the surface of the solid particle has also been suggested [17,18].

Suppression effectiveness should scale with particle surface area for most suppression modes associated with powders. These include heat transfer, radiation, decomposition/vaporization, and surface catalysis. Plots of extinction mass concentration as a function of average particle diameter and surface area can be found in Figures 5a and 5b, respectively, for both bicarbonates in the medium strain rate flames. Average particle surface areas were calculated using average particle diameters. Figure 5a shows that, in the medium strain rate flame, extinction mass concentration increases with diameter, although not linearly. However, as seen in Figure 5b, there does appear to be a linear correlation between extinction mass concentration and average particle surface area at this strain rate.

For the high and low strain rate cases, it was difficult to identify a relationship between extinction effectiveness and either particle size or nominal surface area. In the low strain rate flames, the largest particles were too large to remain suspended in the flow field, and fell directly through the flame into the bottom tube. The dramatic drop off in effectiveness observed in Figure 3 for the two largest particle bin sizes may have resulted from the reduced residence times near the flame. For the high strain rate case, the amount of powder required to extinguish the flame was so small that particle delivery rates were difficult to accurately quantify and control, leading to large uncertainties. Hence, for both high and low strain cases, a large amount of scatter was evident on plots of effectiveness versus particle diameter or surface area. Nevertheless, effectiveness appeared to correlate more closely with surface area than diameter.

Surface area in this study was determined assuming a given sieve fraction could be represented by a spherical particle, with diameter equal to the average of the bin limits. A more accurate determination of the effect of surface area on suppression requires direct measurement of surface area, by gas adsorption for example. More monodisperse powders should also be used. The

extinction results obtained for the 1-D flames of uniform strain rate are consistent with "real world" observations that smaller particles are preferable for suppression purposes, presumably due to the increased surface area [3]. However, any dependence of effectiveness on surface area does not shed light into the primary means by which powders extinguish fires, as all of the suppression modes in operation are interrelated.

In addition to revealing the effects of strain rate, particle size and surface area on suppression effectiveness, Figures 2, 3 and 5 show that KHCO_3 is approximately 2.5 times more effective at extinguishing the flames studied than NaHCO_3 on a mass basis. On a molar basis, potassium bicarbonate is 3 times more effective. The difference in effectiveness between sodium and potassium is partially due to differences in decomposition temperatures and enthalpies, and possibly to differences in catalytic scavenging cycles between the two elements Na and K.

At elevated temperatures, the alkali metal bicarbonates undergo an endothermic decomposition process, releasing carbon dioxide. The residual metal hydroxides vaporize and decompose at much higher temperatures. KHCO_3 decomposes between 100 and 200 °C, whereas NaHCO_3 decomposes at approximately 270 °C. Thus, under similar strain rate conditions and for similar particle size distributions, KHCO_3 requires less time to reach its decomposition phase than NaHCO_3 . Furthermore, according to data compiled by Ewing, Hughes, and Carhart [10], reaction heat sinks associated with decomposition, vaporization and dissociation are reported to be 59.7 kcal/mole and 128.6 kcal/mole for NaHCO_3 and KHCO_3 respectively, assuming the bicarbonates do not decrepitate in the flame. Based on the assumed thermochemistry, KHCO_3 is therefore expected to be more effective in extinguishing the flame than NaHCO_3 for all particle sizes.

The sensible heat capacities associated with bringing the two bicarbonates from ambient temperature to the extinction temperature of a methane flame are reported by Ewing, Hughes, and Carhart [10] to be 57.3 kcal/mole and 47.2 kcal/mole for NaHCO_3 and KHCO_3 , respectively. These heat capacities are tailored to take into account decomposition of the original substances and heat capacities of the decomposition products. For the temperature increase considered, the NaHCO_3 system does have slightly more sensible heat capacity than the KHCO_3 system. However, in their solid states, the two bicarbonates have similar heat capacities. If the delivered particles never reached their decomposition temperatures, in the case of large particles with short residence times in the flame zone for example, NaHCO_3 would be expected to have the same extinction mass concentration as KHCO_3 , assuming surface reactions did not occur.

Flame extinguishment by dry chemical agents is due to a combination of both thermal and chemical mechanism. The relative contribution of each is difficult to determine. Both mechanisms rely on the degradation of the solid particles to have a maximum effect on the flame. The degree of degradation is a function of the particle size which also determines the trajectories of the particles in and near the flame. Smaller particles decompose faster. The enhanced degradation increases suppression effectiveness through greater heat abstraction by highly endothermic processes, such as decomposition and vaporization; and greater production of gas phase atoms, which promote scavenging of important chain branching radicals. The location at which heat is extracted from the flame in the flow field is most likely less important than where chemical players relevant to suppression (if any) are released.

SUMMARY

We have examined the fire suppression properties of bicarbonate powders in propane/air diffusion flames. KHCO_3 was found to be more effective on a mass basis than NaHCO_3 for all

particle sizes tested. It was shown that the effectiveness of bicarbonate powders varies with strain rate, but inversely with particle size in the size range tested: smaller particles are more effective in suppressing the flame than larger ones. Models addressing the behavior of particles in counterflowing fields are consistent with the suppression effectiveness trends observed when the fuel is supplied through the bottom burner tube. Further studies to examine the consequences of delivering the fuel from the top tube, and air and powder from the bottom tube, are planned. The results of these studies will be used to gain a better understanding of flame extinguishment by dry chemicals, and to help determine the characteristics of the optimum agent.

REFERENCES

- [1] Sheinson, R.S., "Fire Suppression by Fine Solid Aerosol," *Proceedings of the International CFC and Halon Alternatives Conference*, Washington, D.C., 24-26 October, 1994, pp. 414-421.
- [2] Hamins, A., Gmurczyk, G., Grosshandler, W., Rehwoldt, R.G., Vazquez, I., Cleary, T., Presser, C., and Seshadri, K., "Flame Suppression Effectiveness," *Evaluation of Alternative In-Flight Fire Suppressants for Full-Scale Testing in Simulated Aircraft Engine Nacelles and Dry Bays*, National Institute of Standards and Testing, No. NIST SP 861, April 1994, pp. 345-465.
- [3] Chattaway, A., Dunster, R.G., Gall, R., and Spring, D.J., "The Evaluation of Non-Pyrotechnically Generated Aerosols as Fire Suppressants," *Proceedings of the Halon Alternatives Technical Working Conference*, Albuquerque, NM, 9-11 May 1995, pp. 473-483.
- [4] Chattaway, A, Gall, R., and Spring, D.J., "Dry Chemical Extinguishing Systems," *Proceedings of the Halon Options Technical Working Conference*, Albuquerque, NM, 6-8 May, 1997, p. 216.
- [5] Dolan, J.E. and Dempster, P.B., "The Suppression of Methane-Air Ignitions by Fine Powders," *Journal of Applied Chemistry*, Sept. 1955, pp. 510-517.
- [6] Rosser, W.A., Inami, S.H. and Wise, H., "The Effect of Metal Salts in Premixed Hydrocarbon-Air Flames," *Combustion and Flame*, 7, June 1963, pp. 107-119.
- [7] Ewing, C.T., Faith, F.R., Hughes, J.T., and Carhart, H.W., "Flame Extinguishment Properties of Dry Chemicals: Extinction Concentrations for Small Diffusion Pan Fires," *Fire Technology*, May 1989, pp. 134-149.
- [8] Fischer, G., and Leonard, J.T., "The Effectiveness of Fire Extinguishing Powders Based on Small Scale Fire Suppressant Tests," *Naval Research Laboratory*, NRL/MR/6180-95-7778, Washington, D.C., 1995.
- [9] Ewing, C.T., Faith, F.R., Romans, J.B., Hughes, J.T., and Carhart, H.W., "Flame Extinguishment Properties of Dry Chemicals: Extinction Weights for Small Diffusion Pan Fires and Additional Evidence for Flame Extinguishment by Thermal Mechanisms," *Journal of Fire Protection Engineering*, 4, 1992, pp. 35-52.
- [10] Ewing, C.T., Hughes, J.T., and Carhart, H.W., "The Extinction of Hydrocarbon Flames Based on the Heat-Absorption Processes which Occur in them," *Fire and Materials*, 8, 1984, pp.148-156.
- [11] Ewing, C.T., Faith, F.R., Hughes, J.T., and Carhart, H.W., "Flame Extinguishment Properties of Dry Chemicals: Extinction Concentrations for Small Diffusion Pan Fires," *Fire Technology*, May 1989, pp. 134-149.
- [12] Knuth, E.L., Ni, W.F., and Seeger, C., "Molecular-Beam Sampling Study of Extinguishment of Methane-Air Flames by Dry Chemicals," *Combustion Science and Technology*, 28, 1982, pp. 247-262.

- [13] Papas, P., Fleming, J. W., and Sheinson, R. S., "Extinction of Nonpremixed Methane- and Propane-Air Counterflow Flames Inhibited with CF_4 , CF_3H , and CF_3Br ", *Twenty-Sixth Symposium (International) on Combustion*, The Combustion Institute, Pittsburgh, 1996, p. 1405.
- [14] Fisher, E.M., Williams, B.A., and Fleming, J.W., "Determination of the Strain in Counterflow Diffusion Flames from Flow Conditions," *1997 Proceedings of the Fall Technical Meeting: The Eastern States Section of the Combustion Institute*, Hartford, CT, (1997), pp. 191-194.
- [15] Li, S.C., Libby, P.A., and Williams, F.A., "Spray Structure in Counter flowing Streams with and without a Flame," *Combustion and Flame*, **94**, 1993, pp. 161-177.
- [16] Lentati, A.M. and Chelliah, H.K., "The Dynamics of Water Droplets in a Counterflow Field and its Effect on Flame Extinction," *1996 Proceedings of the Fall Technical Meeting: The Eastern States Section of the Combustion Institute*, Hilton Head, SC, (1996), pp. 281-284.
- [17] Dewitte, M., Vrebosch, J. and van Tiggelán, A., "Inhibition and Extinction of Premixed Flames by Dust Particles," *Combustion and Flame*, **8**, (1964), p. 257.
- [18] Seeger, P.G., "A Laboratory Test Method for Evaluating the Extinguishing Efficiency of Dry Powder," *AGARD Conference Proceedings*, Vol. 166, Paper 24 (1975)
- [19] Williams, B.A., Fleming, J.W., and Sheinson, R.S., "Extinction Studies of Hydrofluorocarbons in Methane/Air and Propane/Air Counterflow Diffusion Flames: The Role of the CF_3 Radical," *Proceedings of the Halon Options Technical Working Conference*, Albuquerque, NM, 6-8 May, 1997, pp. 31-42.

Table 1: Flow and strain rate conditions for extinction experiments

	Nominal Strain rate		
	High	Medium	Low
Air Flow Rate (SLPM)	3.5	2.4	1.5
Fuel Flow Rate (SLPM)	2.8	1.7	1.0
Global Strain rate ^a (sec ⁻¹)	290	180	110
Measured Strain rate (sec ⁻¹)	475	305	180

a - Calculated strain rate following Fisher, Williams, and Fleming [14]

Table 2: Propane-air counterflow diffusion flame extinction mass concentration for the indicated agent. Halon 1301 data derived from Ref. [19].

Chemical	Measured Strain rate (s ⁻¹)	Extinction Mass Concentration for Specified Size Bin (g/m ³)				
		<38 μm	38-45 μm	45-53 μm	53-63 μm	63-75 μm
NaHCO ₃	180	70	52	150	270	730
	310	8	15	53	56	80
	480	4	1	7	7	4
KHCO ₃	180	12	18	70	100	370
	310	3	12	20	18	51
	480	1	6	3	1	2
Halon 1301	180	110				
	310	56				
	480	15				

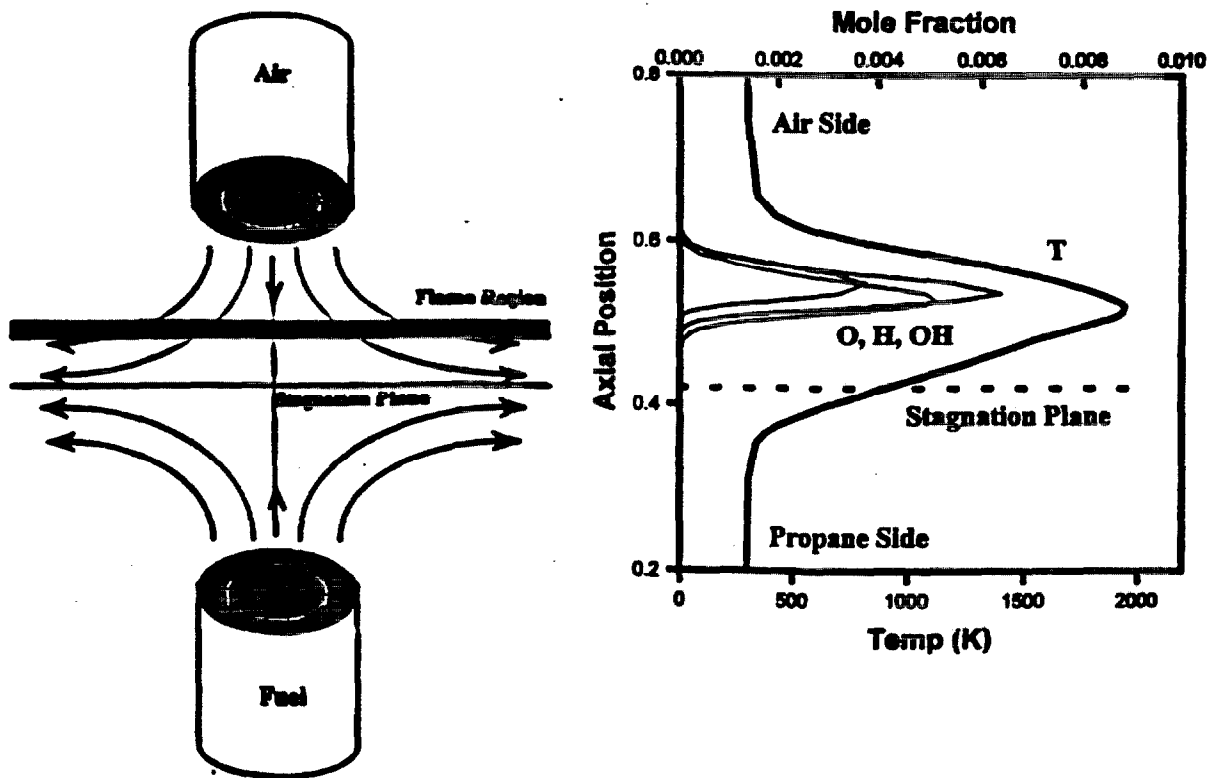


Figure 1: Schematic of the counterflow diffusion burner showing air on top and propane on bottom and calculated temperature, O, H, and OH profiles for the low strain flame.

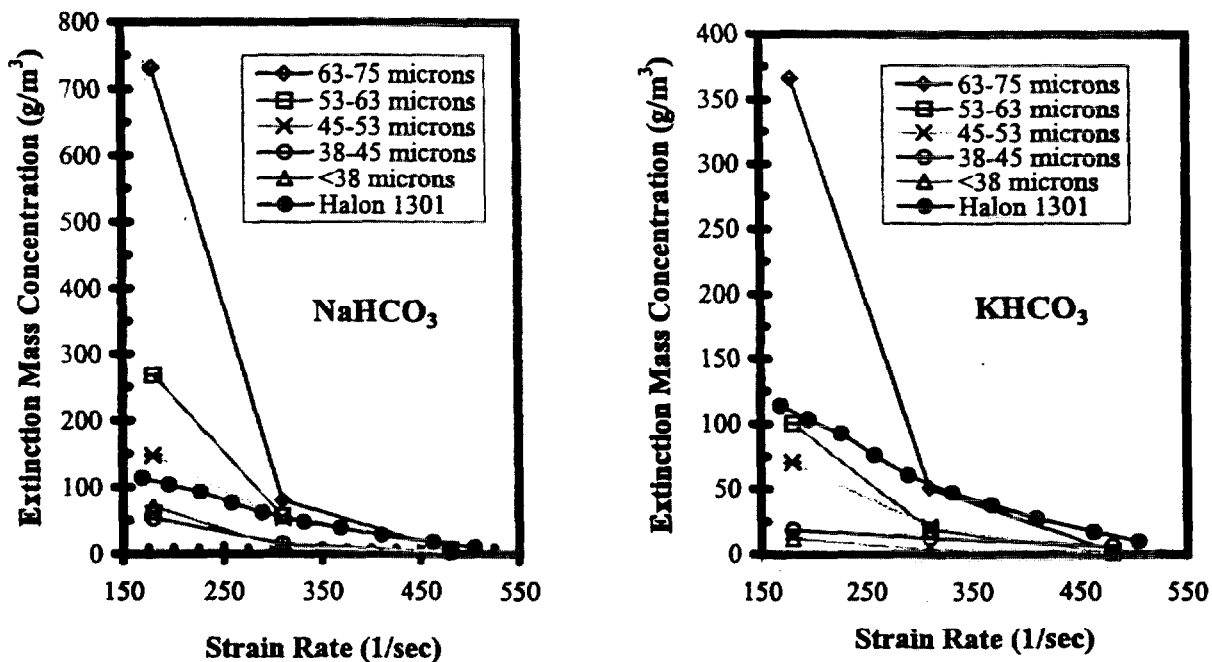


Figure 2: Extinction mass concentration as a function of strain rate for each particle size range of (a) NaHCO_3 and (b) KHCO_3 powders in a propane/air counterflow diffusion flame. Halon data from Reference [19].

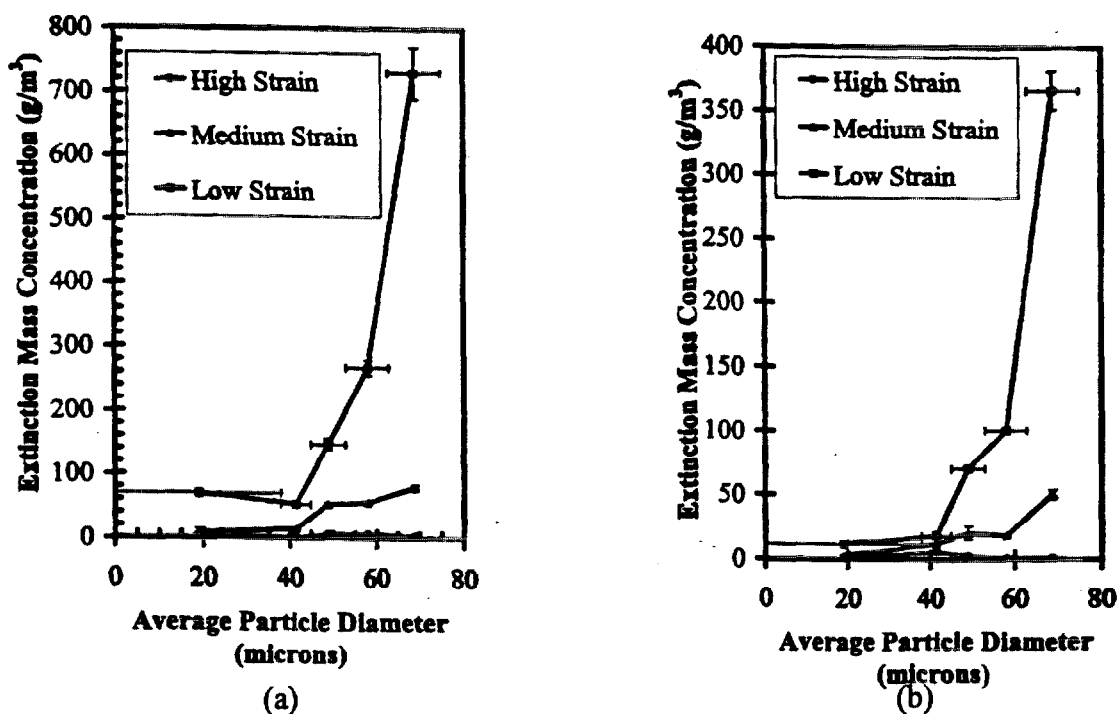


Figure 3: Same data as Figure 2 replotted to show extinction mass concentration as a function of particle size range for each strain rate propane/air counterflow diffusion flame and added (a) NaHCO_3 and (b) KHCO_3 powder.

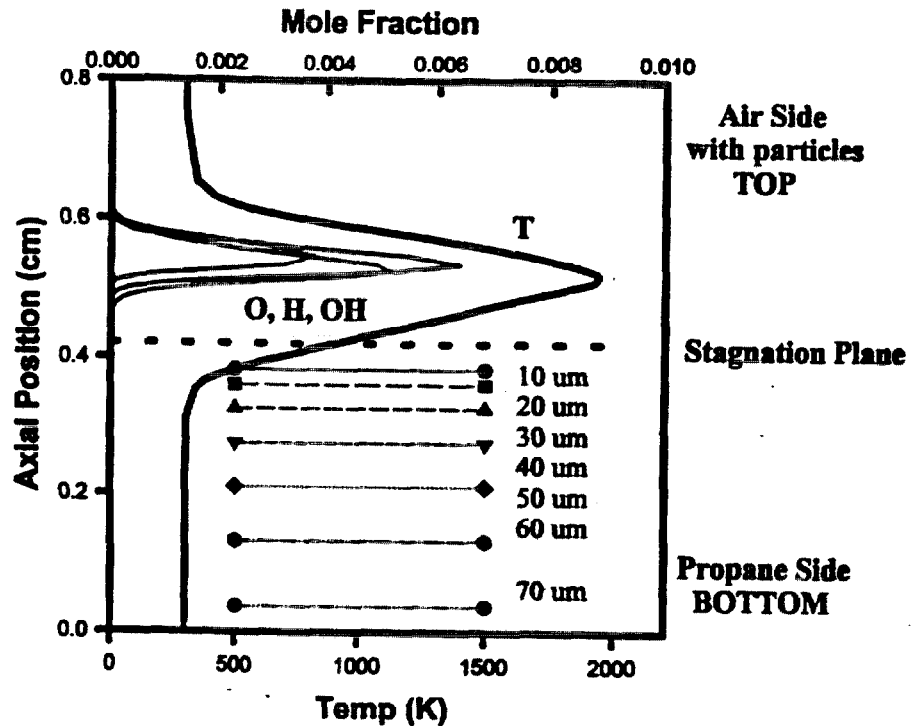


Figure 4: Calculated particle asymptotic location as a function of particle diameter for the flow conditions of the low strain propane/air flame.

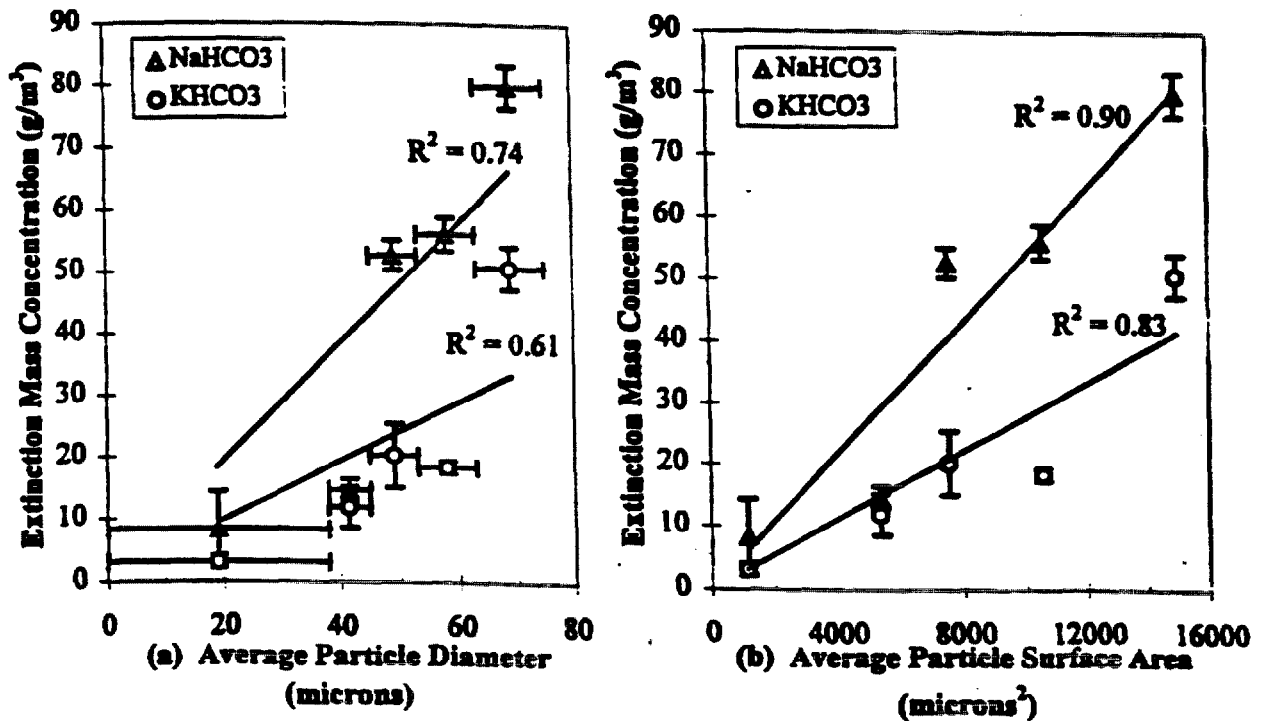


Figure 5. Extinction mass concentration as a function of (a) average particle diameter of the indicated size range and (b) average particle surface area for NaHCO_3 and KHCO_3 powders in a medium strain rate (310 s^{-1}) propane/air counterflow diffusion flame.